Processing and Application of Ceramics 10 [3] (2016) 189–198

DOI: 10.2298/PAC1603189V

Degradation of crystal violet over heterogeneous TiO_2-based catalysts: The effect of process parameters

Marija B. Vasić[1], Marjan S. Randjelović[1], Milan Z. Momčilović[2], Branko Z. Matović[2], Aleksandra R. Zarubica[1,*]

[1]*Department of Chemistry, Faculty of Science and Mathematics, University of Niš, Višegradska 33, 18000 Niš, Serbia*

[2]*"Vinča" Institute of Nuclear Sciences, Materials Science Laboratory, University of Belgrade, P.O. Box 522, Belgrade, Serbia*

Received 23 May 2016; Received in revised form 23 August 2016; Received in revised form 23 September 2016; Accepted 27 September 2016

Abstract

In this study, modified sol-gel method was employed to synthesize the pure and Zr-doped titania catalysts. Brunauer-Emmett-Teller (BET) method was applied to determine porosity, X-ray diffraction (XRD) analysis was used to study crystal structure, scanning electron microscopy (SEM) was used to investigate morphology and Fourier transform infrared spectroscopy (FTIR) was used to examine surface properties/total acidity of the obtained catalysts samples. Photocatalytic activity was tested in the reaction of crystal violet (CV) dye decolourization/degradation under UV light irradiation. The effects of several photocatalysis operational parameters were considered, such as catalyst dosage, initial dye concentrations, duration of UV irradiation treatment, as well as catalysts calcination temperatures and dopant amounts. The obtained results indicated faster dye decolourization/degradation with the increase of the catalyst dosage and the decrease of initial CV concentrations. The Zr-doping affects photocatalytic properties, i.e. CV decolourization/degradation of the prepared catalytic materials. Thus, addition of 5 wt.% of ZrO_2 to titania increases photocatalytic effect for ~15% and addition of 10 wt.% of ZrO_2 improves the photocatalytic efficiency of titania for nearly 30%.

Keywords: *titania, Zr-doping, nanopowders, heterogeneous catalysts, photocatalytic activity*

I. Introduction

The presence of dyes in waste water originally comes from textile and other industries, which presents a worldwide environmental danger and one of the crucial problems that modern science is confronting nowadays [1]. Crystal violet is triphenylmetane dye, which is widely used in paper, leather and printing industry. It can be carcinogenic, toxic and mutagenic for water organisms and mammalian cells [2,3].

Traditional methods, such as thermal destruction [4,5], biodegradation [6] and various adsorption processes [7,8], are ineffective for removal of organic pollutants. Biological treatments take too much time, thermal treatments are energetically inefficient, while adsorption processes comprise mass transfers of reactants and/or products over (surfaces) interfaces [6].

Heterogeneous photocatalysis is one of the most promising (new) technologies for waste water treatments, especially if organic pollutants (dyes) are present [9]. Due to its numerous favourable properties, TiO_2 has many applications and it is one of the most commonly used photocatalysts in processes connected with environmental protection [1]. The titania-based catalyst is both chemically and biologically inert, stable under a wide range of conditions, noncorrosive, nontoxic and highly active [10]. Titania can be prepared by conventional sol-gel method, the process which is relatively fast and cost-effective and simultaneously produces a catalyst characterized with favourable properties [11].

It has been reported that doping of titania with a variety of transition metals results in surface modifica-

*Corresponding author: tel: +381 63 11 18 55, fax: +381 18 533 014, e-mail: *zarubica2000@yahoo.com*

tion and formation of crystal defects, which can lead to significant improvement in its photocatalytic properties. Zirconium has been successfully used as a dopant for titania, which can be ascribed to the fact that Ti and Zr belong to the same group of elements and their tetravalent cations have comparable ionic radii [12]. In addition, relevant oxides of both elements (TiO_2 and ZrO_2) are n-type semiconductors with similar physico-chemical properties, which probably lead to their interaction during catalyst preparation [13].

To the best of our knowledge, there are no studies reporting synthesis of Zr-doped titania via modified sol-gel method using zirconium(IV) oxychloride octahydrate as a precursor, while only a few papers investigated the influence of doping on catalyst activity of titania and photocatalytic reactions of degradation/decolourization of the selected organic dye [11,12,14–16]. The present study reports economical and environmentally friendly method for obtaining TiO_2-based powders by using modified sol-gel method. Additionally, the influence of Zr-doping on physico-chemical properties (and activity) of titania was investigated. Decolourization/degradation of cationic dye CV under UV light irradiation was used as a test reaction for the purpose of investigating the activity of catalysts. In addition, impacts of several photocatalysis process parameters on the (photocatalytic) performance of the pure and Zr-doped TiO_2 were studied, including catalyst dosage, duration of irradiation treatment, initial dye concentrations, as well as different calcination temperatures of catalysts and dopant amounts in the catalyst preparation procedure.

II. Experimental

2.1. Catalyst preparation

TiO_2-based catalysts were synthesized via modified sol-gel method using titanium isopropoxide (Aldrich Co.) as a precursor. In the first step two solutions were prepared. The first solution was made by dissolving the calculated/measured amount/volume of titanium isopropoxide in 2-propanol according to stoichiometry under inert conditions. Then, the second solution was made by mixing water and 2-propanol in volume ratio 1 : 3 which was added to the first solution drop by drop under vigorous stirring in nitrogen atmosphere for one hour. The molar ratio Ti : H_2O was adjusted to 1 : 6 and pH of the resulting suspension to 10 by 1 M NaOH. The obtained precipitate was filtered, washed with distilled water and finally with the mixture of isopropanol and water. After that, the powder sample was dried at 105–110 °C for 3 h, and then calcined for additional 3 h at different temperatures of 450, 600 and 800 °C. The catalytic sample was heated to the desired temperature at a heating rate of 10 °C/min. All chemical reagents were applied as received from commercial source (analytical purity) without further purification.

The Zr-doped samples were prepared by using $ZrOCl_2 \cdot 8\,H_2O$ (Sigma Aldrich, Co.) diluted in distilled water. Three doped titania samples were obtained by adding 2.5, 5.0 and 10.0 wt.% of ZrO_2. After drying for 3 h at 105 °C, the doped catalysts samples were calcined at two different temperatures (600 and 800 °C) for 3 h, using the heating rate 10 °C/min. The used chemicals were of analytical grade and no additional purification was performed. The obtained catalysts were denoted as: X-Zr-TiO_2-T, where X stands for the amount in wt.% of added ZrO_2 and T for calcination temperature.

2.2. Catalyst characterization

In order to determine the specific surface area and porosity of catalyst, BET and Barett-Joyner-Halenda (BJH) methods were used, respectively. XRD method was used for characterization of catalyst structure, and the surface morphology was estimated by SEM. FTIR method was used for evaluation of surface properties of catalysts, i.e. determination of Lewis (LAS) and Brønsted acid sites (BAS) as catalytically active sites.

BET surface area measurements were performed on a Micromeritics ASAP 2010 based on adsorption/desorption of liquid nitrogen at appropriate temperature and pressure (LTN_2AD) by He as carrier gas. The average pore diameters and pore volumes were determined by BJH method. Prior to measurements, all catalyst powder samples were degassed.

XRD analysis was carried out on a Philips APD-1700 diffractometer using Cu-anticathode and monochromator in operating mode of 40 kV and 55 mA. Data were collected in the 2θ scan range between 10 and 80°. The average crystallite sizes were calculated by using Scherrer equation [17]:

$$d = \frac{k \cdot \lambda}{\beta \cos\theta} \tag{1}$$

where λ is X-ray wavelength, k is constant 0.9, β is the peak width at half maximum, and θ is the Bragg angle. The weight fraction of anatase (W_A) in the powder was calculated by the following equation developed by Spurr *et al.* [18,19]:

$$W_A = \frac{1}{1 + 1.265\frac{I_R}{I_A}} \times 100 \tag{2}$$

where I_A and I_R are (integrated) peak intensities of the most intense peaks for anatase 101 and rutile 110 peaks/phases, respectively.

The surface morphology of the catalysts was investigated by scanning electron microscope SEM JOEL JSM-6460LV. Sample preparation for SEM imaging was performed by coating with gold layer. Operating conditions in SEM imaging were: acceleration voltage 25 kV, 30 mA current at a working distance of 50 mm during 180 s.

In order to evaluate catalyst surface acidity, FTIR analysis was carried out by KBr pellet technique. FTIR spectra measurements before and after pyridine adsorption were recorded on a Win Bomem Easy spectrome-

ter with 2 cm^{-1} resolution in the scanning range between 4000 and 400 cm^{-1}.

2.3. Photocatalytic activity

In order to test photocatalytic activity of the catalysts, degradation of crystal violet (CV) dye was tested under irradiation of UV lamp (Roth Co., 16 W, 2.5 mW/cm^2, with maximal emission at 366 nm). The UV lamp was located at a distance of 10 cm from the reaction model solution, which was magnetically stirred during the experiments with a constant speed. CV dye solution (10 ml) was placed in quartz reaction tube covered with 0.5 mm thick quartz disk-cover, and then irradiated with UV light.

Before UV illumination, catalysts had been mixed with crystal violet test-solution at constant stirring during 24 h in dark in order to establish adsorption-desorption equilibrium of dye molecules onto the catalysts surface. This was performed in order to avoid adsorption of CV dye on the catalysts surfaces during the photocatalytic reaction. The decolourization/degradation process was monitored by measuring maximal absorbance of CV solution (at λ_{max} = 590 nm) using UV/Vis spectrophotometer (Schimadzu Co.). At specified time-intervals, aliquots were withdrawn from the solution, then centrifuged and filtrated before measuring.

III. Results and discussion

3.1. Textural properties

The textural properties (nitrogen adsorption-desorption isotherms, pore size distribution curves, BET specific surface area, average pore diameter and pore volume) of the pure and Zr-doped titania powders calcined at different temperatures are presented in Figs. 1 and 2 and summarized in Table 1. All samples were calcined at selected temperatures (i.e. 600 and 800 °C) in order to incorporate zirconium into titania according to recently reported data [6,11,13].

Table 1. Textural properties (specific surface area S_{BET}, mean pore diameter d_p, pore volume V_p) of titania-based catalysts samples

Sample	S_{BET} [m^2g^{-1}]	d_p [nm]	V_p [cm^3g^{-1}]
TiO_2-450	34.3	8.3	0.075
TiO_2-600	28.1	11.2	0.070
TiO_2-800	22.4	13.7	0.065
2.5-Zr-TiO_2-800	10.1	28.9	0.057
5-Zr-TiO_2-600	40.6	6.5	0.088
5-Zr-TiO_2-800	37.4	7.7	0.072
10-Zr-TiO_2-600	46.8	5.3	0.099
10-Zr-TiO_2-800	43.3	6.1	0.083

In general, all investigated catalytic samples exhibited type IV sorption isotherm curves, which indicated the presence of mesoporosity accompanied with possible capillary condensation of adsorbent in gaseous and/or liquid phase. The nitrogen adsorption/desorption isotherm curves of the pure and Zr-doped titania are shown in Figs. 1a and 1b, respectively. The pure titania catalysts samples calcined at selected temperatures exhibit typical *S*-shape behaviour of type IV sorption isotherm with a type H1 hysteresis loop, while the Zr-doped titania samples calcined at selected temperatures were characterized with type IV sorption isotherm with a type H3 hysteresis loop according to IUPAC classification [20,21].

These observations are typical for mesoporous materials. The noticed hysteresis loops indicate the presence of mostly cylindrical pore shapes in the pure titania sample, while the Zr-doped titania samples have cracks-like and/or conical pores. The isotherms of the doped titania catalytic samples were shifted slightly downward, and their hysteresis loops were shifted to rather higher relative pressures. The incorporation of higher amount of dopant into titania caused shifts of hysteresis loops to somewhat higher relative pressures (not shown). The application of higher calcination temperatures for the Zr-doped titania shifts the hysteresis loops to moderately

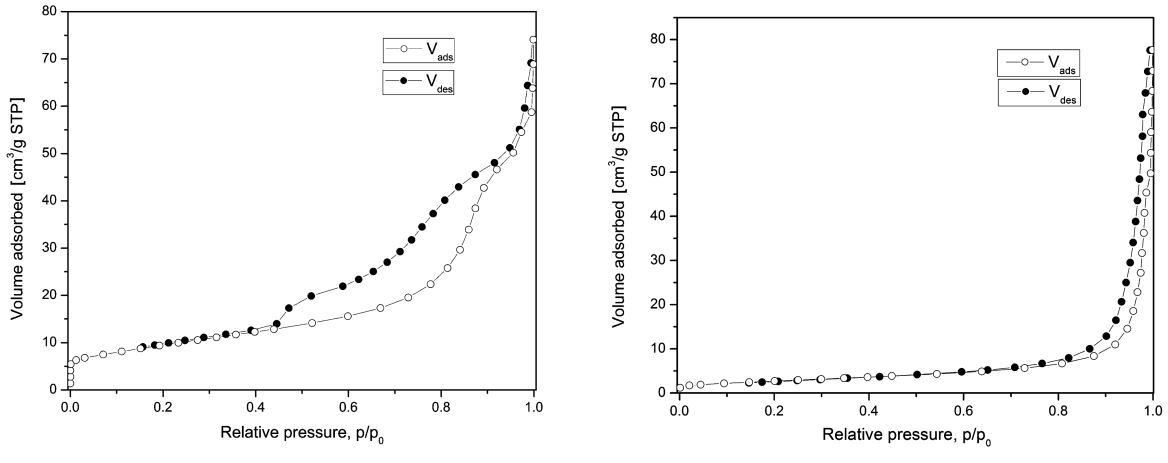

Figure 1. Nitrogen adsorption-desorption isotherm for: a) TiO_2-450, b) 2.5-Zr-TiO_2-800 samples

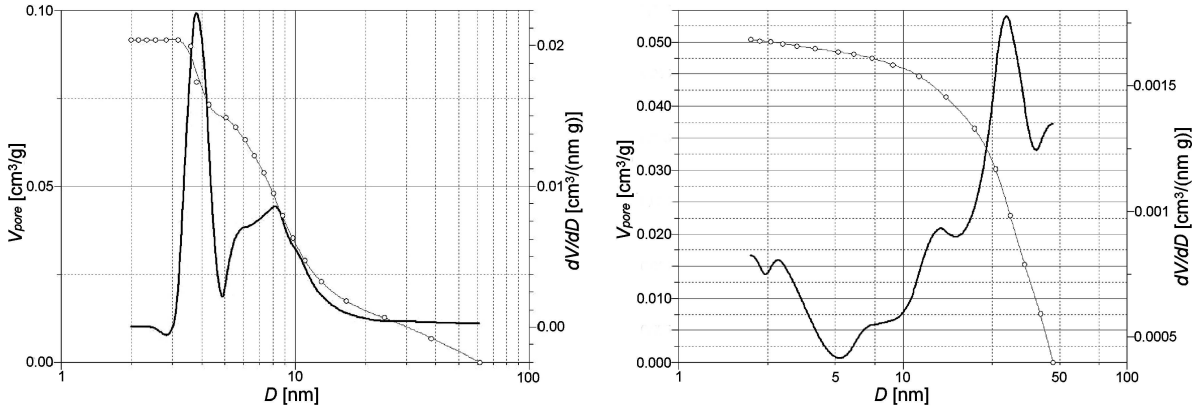

Figure 2. Pore size distribution of: a) TiO_2-450, b) 2.5-Zr-TiO_2-800 samples

higher relative pressures (not shown). These changes are in agreement with a fact that specific surface area of the doped titania catalysts increases with the increase of Zr amount (Table 1).

Figure 2 shows the pore size distribution of the titania-based catalytic samples. The bimodal pore sizes distributions in the pure titania samples show that all TiO_2 catalysts have two types of pores: micropores or pores at (near-edge) micro-meso pore boundary, and typical mesopores characterized with the average pore diameter of about 8 nm (Fig. 2a). The doped titania catalytic samples are characterized with atypical bimodal or multi-modal distributions of pore sizes. Consequently, the catalytic Zr-doped titania samples have at least two different pore sizes: micropores, probably presented as interstices among titania primary crystallites, and mesopores, characterized with the average pore diameter of 45 nm probably associated with interstices among secondary crystallites and relatively poorly dispersed dopant (Fig. 2b). It is important to note that somewhat higher volume of mesopores with greater average pore size is observed in the case of the doped titania powders. The incorporation of higher Zr-amount causes the existence of bimodal and/or multimodal pore size distribution typical for the revealed materials mesoporosity. Volume fraction of mesopores characterized with greater average pore diameter fairly increased with the increase of zirconia weight percentage. The increase of calcination temperature affected a shift of maxima in pore size distribution curves to mesopores with larger average pore diameter, and their volume ratios slightly increased (not shown).

The estimated BET surface area of the pure titania catalyst sample calcined at 450 °C is 34.3 m^2/g (Table 1), which is slightly smaller than previously reported [22]. Doping of titania with 5 and 10 wt.% of ZrO_2 results in somewhat larger pore volumes and specific surface areas. In addition, the specific surface area and pore volume of the doped samples increase with Zr-content (Table 1). The observed behaviour can be explained by initial sintering during calcination at elevated temperature or inhomogeneous dispersion of Zr^{4+} ions.

3.2. Microstructural characterization - XRD

Figure 3 shows XRD patterns of the pure and Zr-doped titania powders after calcinations at different temperatures. All diffraction peaks of the pure titania calcined at 450 °C are characteristics of exclusively anatase crystal phase (Fig. 3a). The XRD pattern of the pure titania calcined at 600 °C has peaks of both anatase and rutile phases, while predominantly rutile crystal phase is present in the sample calcined at 800 °C.

However, the XRD pattern of the doped titania sample 5-Zr-TiO_2-600, calcined at 600 °C, shows peaks characteristic of titania anatase phase, negligible fraction of rutile phase and probably a small amount of brookite titania phase (Fig. 3b). Whereas, the XRD pattern of the sample 5-Zr-TiO_2-800, calcined at 800 °C, shows peaks typical for both anatase and rutile phases as well as probably some traces of monoclinic and/or tetragonal zirconia phase. The addition of 5 wt.% ZrO_2 resulted in slighter retarding of anatase-to-rutile phase transformation at elevated temperatures (Fig. 3b). The increase of calcination temperatures and addition of ZrO_2 also improved the crystalline structure of the photocatalyst, which is confirmed with stronger and sharper XRD peaks (Fig. 3). The authors were not able to identify only few weak peaks appearing after doping.

The XRD pattern of the doped titania catalyst sample 10-Zr-TiO_2-600 calcined at 600 °C displays peaks characteristic of titania anatase phase, and probably a small amount of brookite titania and/or monoclinic/tetragonal zirconia phases (Fig. 3b). Moreover, the XRD pattern of the doped titania sample 10-Zr-TiO_2-800 calcined at 800 °C shows peaks typical for both anatase and rutile phases and probably a small amount of $ZrTiO_4$ and/or monoclinic zirconia phase. The addition of 10 wt.% ZrO_2 resulted in noticeable retarding of anatase-to-rutile phase transformation at elevated temperatures (Fig. 3b).

Having in mind that ionic radius of Zr^{4+} ion (0.072 nm) is somewhat larger than one of Ti^{4+} ion (0.053 nm) [23], it is expected that Zr^{4+} ions could re-

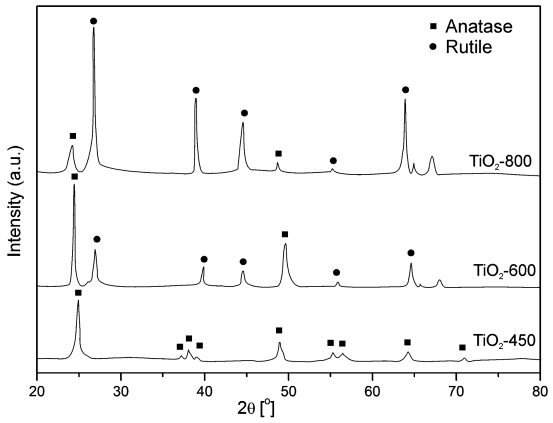

(a)

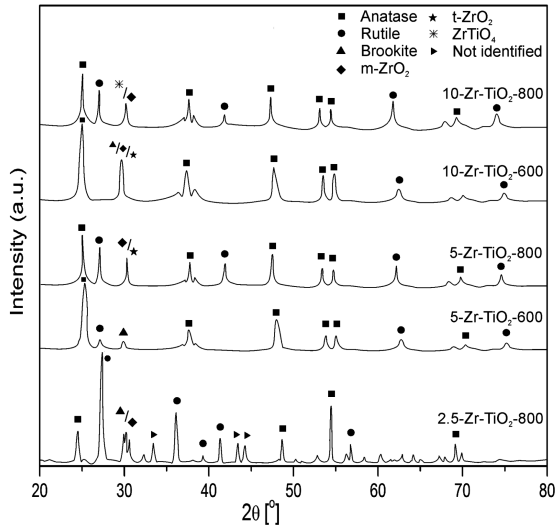

(b)

Figure 3. XRD patterns of: a) TiO_2-450, TiO_2-600, TiO_2-800, and b) 2.5-Zr-TiO_2-800, 5-Zr-TiO_2-600, 5-Zr-TiO_2-800, 10-Zr-TiO_2-600, 10-Zr-TiO_2-800 samples (anatase, rutile and brookite peaks were compared to the data from JCPDS file No. 21-1272, JCPDS file No. 21-1276 and 29-1360, respectively)

place Ti^{4+} in the titania lattice. This should cause a XRD shift of titania to somewhat lower diffraction angles in comparison to the pure titania. It is observed (Fig. 3.) that the diffraction peaks of anatase and rutile phases in the doped titania catalysts are gradually shifted to lower angles compared to the pure titania. This is additional confirmation that Zr^{4+} ions enter into the titania lattice substituting Ti^{4+} ions. The registered new diffraction peak of $ZrTiO_4$ in the doped titania 10-Zr-TiO_2-800 sample indicates that the substitution of Ti^{4+} with Zr^{4+} ions in titania becomes saturated at 800 °C and when Zr^{4+} ions increase to the appropriate content.

In general, addition of 10 wt.% ZrO_2 cause retarding the anatase-to-rutile phase transformation and growth of anatase crystallites at elevated temperatures.

Phase composition of titania-based materials is very important as initial research in the topic indicating that photocatalytic activity was related to the existence of the single anatase phase [24], but following studies point out to the importance of both anatase and rutile crystal phases for photocatalytic activity of the titania-based materials [25–27]. It was also reported [28] that a mixture of anatase, rutile and brookite phases exhibits higher photocatalytic activity than single anatase phase.

3.3. Microstructural characterization - SEM

Figure 4 shows the SEM images of the pure and Zr-doped titania samples. The SEM image of the pure titania TiO_2-800 sample calcined at 800 °C shows typical spherical morphology consisting of small primary particles. The presence of interparticles pores can be easily observed (Fig. 4a). After Zr-doping morphology of the calcined particles is completely changed (Fig. 4b). A lot of fine particles with specific morphology are observed in the Zr-doped titania. This is confirmed with the observed increase of the specific surface area of the doped titania samples (Table 1).

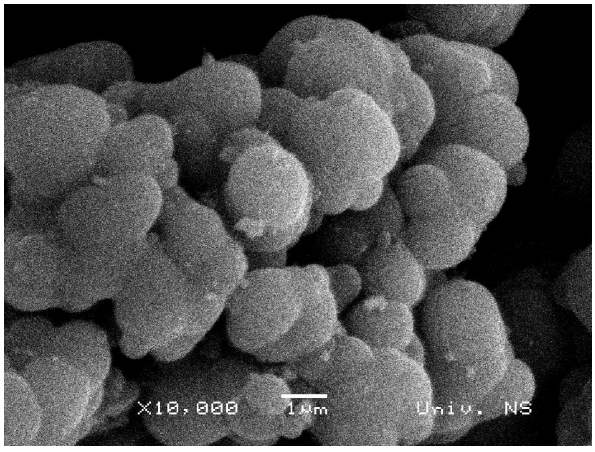

(a)

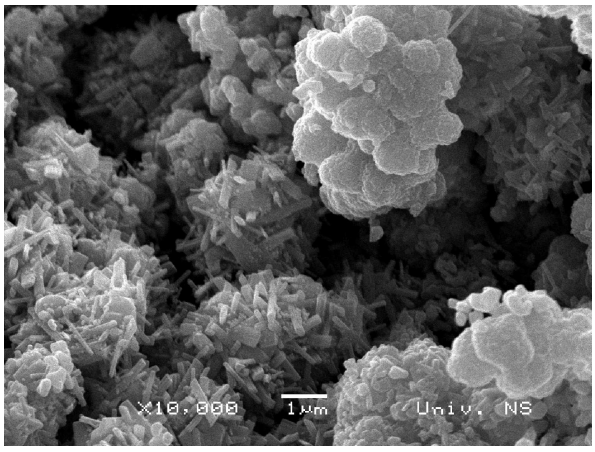

(b)

Figure 4. SEM micrographs of catalyst samples: a) TiO_2-800 and b) 10-Zr-TiO_2-800

3.4. Microstructural characterization - FTIR

FTIR spectrum of the pure titania (calcined at 450 °C) after pyridine adsorption is presented in Fig. 5a. The

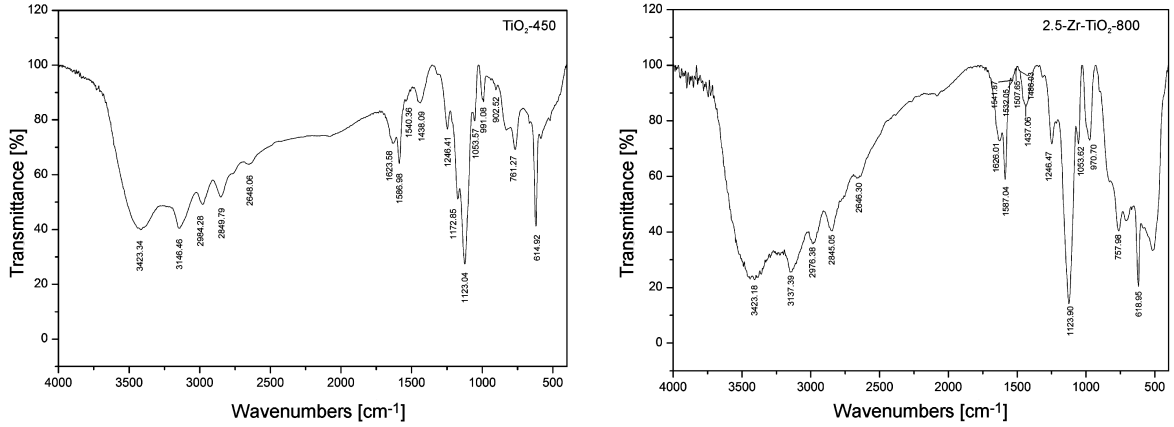

(a) (b)

Figure 5. FTIR spectra of catalyst samples: a) TiO_2-450, b) 2.5-Zr-TiO_2-800 samples

peaks for Lewis acid sites (LAS) at 1624, 1587 and 1438 cm^{-1} are present, along with peaks for Brønsted acid sites at 1540 cm^{-1}. The band at 1540 cm^{-1} is the characteristic for pyridinium cation and is formed as a result of pyridine interaction with Brønsted acid sites (Fig. 5a) [29].

According to FTIR spectra, the calcined Zr-doped titania is characterized with increased intensity of the LAS at 1438 cm^{-1}, 1587 and 1626 cm^{-1} compared with counterpart bands of the pure titania (Fig. 5). This indicates on a slightly greater number of the Lewis acid sites on the surface of the doped titania (Fig. 5b). The bands around 1540 cm^{-1} in both catalytic samples have similar intensity, so both catalyst samples probably possess comparable number of Brønsted acid sites. Broad adsorption band around 3423 cm^{-1} is present in both catalysts samples. This band originates from the stretching vibration of titania surface hydroxide groups and molecularly adsorbed water and can also act as a weak surface catalytically active site. A band characteristic of pyridine hydration at around 1120 cm^{-1} specific for the hydrated titania anatase crystal phase is present in both samples, but has a higher intensity in the case of the Zr-doped titania [29].

3.5. Photocatalytic activity

Influence of dopant amount and calcination temperature

The pure titania catalyst calcined at 600 °C showed high photocatalytic activity after CV degradation of around 20 h under relatively mild conditions (low UV radiation energy, natural pH). The pure titania catalyst calcined at 800 °C presented somewhat lower photocatalytic activity in comparison with the catalyst calcined at 600 °C under the same conditions (not shown).

Favourable photocatalytic activity of the titania samples can be ascribed to acceptable BET specific surface area and pore volume, the presence of highly catalytically active anatase crystal phase, and total surface acidity of titania. The photocatalytic CV degradation is improved over the Zr-doped titania because of its improved physico-chemical properties and improved mechanism of CV decolourization/degradation process compared to the pure titania. Namely, the Zr-doped titania has bimodal/multimodal distribution of pore sizes in comparison to bimodal-pore size distribution in the case of the pure titania powder. Bimodal/multimodal pore size distribution can enable reactant(s) to more easily reach the catalytically active sites. In addition, sufficiently large pore volume facilitates an easier transport of reactant(s) to the catalytically active sites, and diffusion of the products back to the reaction mixture [30].

The incorporation of zirconium into titania caused the formation of particles with larger specific surface areas and pore volumes in comparison to their pure counterparts except for 2.5-Zr-TiO_2-800 (Table 1). The achieved photocatalytic activity of the Zr-doped titania catalysts increased with the increase of of Zr-content (Fig. 6). In general, all physico-chemical properties of

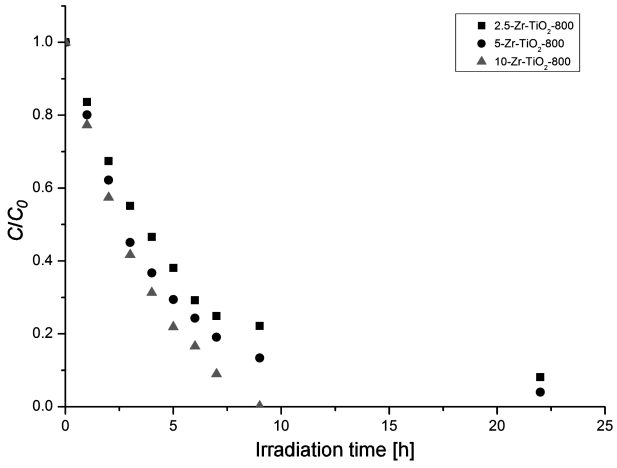

Figure 6. Influence of dopant amount on photodegradation rate of Zr-doped titania samples calcined at 800 °C (catalyst amount 0.05 g, initial CV dye concentration 0.01 mmol/dm^3, pH = 6.7 to 7.0)

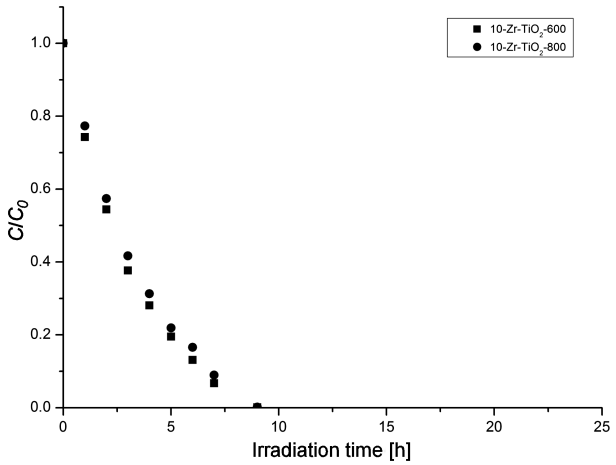

Figure 7. Influence of calcination temperatures on photodegradation rate of 10-Zr-TiO_2-600 and 10-Zr-TiO_2-800 samples (catalyst amount 0.05 g, initial CV dye concentration 0.01 mmol/dm^3, pH = 6.7 to 7.0)

the Zr-doped titania were improved with the increase of Zr-content. These improvements highly affected their photocatalytic performances and resulted in superior photocatalytic ability of catalysts 10-Zr-TiO_2-600 and 10-Zr-TiO_2-800 in CV degradation (Figs. 6 and 7).

The authors confirmed, similarly to other literature reports, that better crystallinity of the Zr-doped titania [26], and presence of titania mixed crystal phases (anatase-rutile-brookite and $ZrTiO_4$) [25–28] improve catalytic efficiency of the Zr-doped titania. Moreover, it is believed that the observed higher total acidity of the Zr-doped titania surface (of the samples 10-Zr-TiO_2-600 and 10-Zr-TiO_2-800) is responsible for better catalytic ability in the process of the photocatalytic degradation of CV [31–34]. In the case of the Zr-doped titania with 10 wt.% of ZrO_2, the increase of the calcination temperature from 600 to 800 °C caused a slight decrease of the photocatalytic activity under the same experimental conditions (Fig. 7.).

We proposed that the incorporation of Zr^{4+} ions into titania can generate additional formation of $O_2^{-\bullet}$ and $^{\bullet}OH$ radicals that can take part in the successive photocatalytic subreactions responsible for CV degradation. The introduction of sufficient amount of Zr^{4+} ions into titania lattice can restrict the recombination rate of photogenerated electrons and holes, thus enhancing the photocatalytic efficiency of the pure titania. In the case of Zr^{4+} ions, the rate of charge carriers (electrons and holes) detrapping is high, which has positive influences on photocatalytic efficiency of the Zr-doped titania. The induced oxygen vacancies by incorporation of Zr^{4+} ions into titania can additionally capture photogenerated electrons thus limiting the charge carriers recombination rate. The generated oxygen vacancies support the process of oxygen adsorption and increase the interaction between photoinduced electrons of oxygen vacancies and adsorbed oxygen favouring photocatalytic reactions and improving adsorption and degradation of CV dye molecules [35]. Oxygen adsorbed onto doped titania after accepting electron is reduced to $O_2^{-\bullet}$, and surface hydroxyl group is converted to hydroxyl radical $^{\bullet}OH$ by an acceptance of hole. Both $O_2^{-\bullet}$ and $^{\bullet}OH$ radicals further assisted CV degradation. Therefore, the introduction of the appropriate amount of Zr^{4+} ions into titania lattice significantly improved photocatalytic activity of the pure titania [35]. With the presence of Zr^{4+} ion in titania lattice, the following reactions are possible [35]:

$$TiO_2 + h\nu(UV) \longrightarrow TiO_2 + e^-_{CB} + h^+_{VB}$$

$$h^+_{VB} + OH^- \longrightarrow {}^{\bullet}OH$$

$$h^+_{VB} + H_2O \longrightarrow {}^{\bullet}OH + H^+$$

$$e^-_{CB} + O_2 \longrightarrow O_2^{-\bullet}$$

$$\text{X-Zr-TiO}_2\text{-T}(Zr^{4+}\text{–TiO}_2) + h\nu(UV) \longrightarrow \text{X-Zr-TiO}_2\text{-T}(Zr^{4+}\text{–TiO}_2) + e^-_{CB} + h^+_{VB}$$

$$Zr^{4+} + e^-_{CB} \longrightarrow Zr^{3+}$$

$$Zr^{3+} + O_2 \longrightarrow Zr^{4+} + O_2^{-\bullet}$$

Influence of catalyst dosage

The influence of catalysts dosages (amounts from 0.030 to 0.075 g) on the CV degradation process is shown in Fig. 8. It can be noticed that concentrations of the selected dye have decreased with the increase of the catalysts amounts when both pure and Zr-doped titania catalysts were used (Fig. 8). Higher amounts of both catalysts mean that there are larger numbers of catalytically active sites as well as larger numbers of adsorbed photons that may result in the enhanced photocatalytic activity.

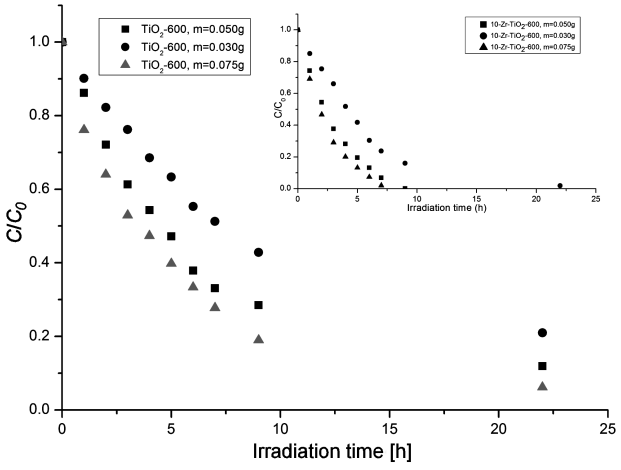

Figure 8. Influence of the catalyst amount (pure TiO_2-600 and doped 10-Zr-TiO_2-600 samples) on photodegradation rate (experimental condition: initial CV dye concentration 0.01 mmol/dm^3, pH = 6.7 to 7.0)

Influence of initial CV concentrations

The effect of initial CV concentrations from 0.005 to 0.010 mmol/dm^3 was investigated for the constant cata-

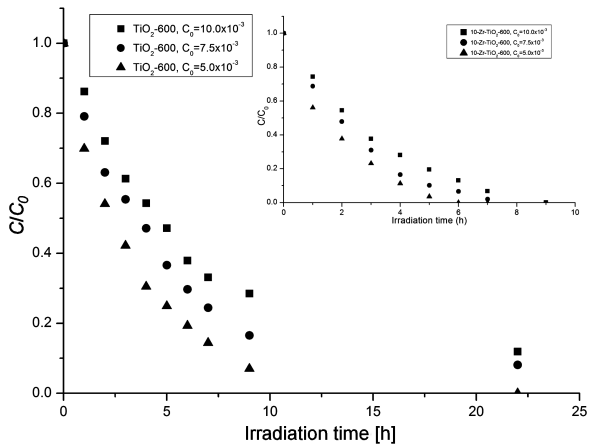

Figure 9. Influence of initial CV dye concentration on photodegradation rate of the pure TiO_2-600 and doped 10-Zr-TiO_2-600 samples (catalyst amount 0.05 g, pH = 6.7 to 7.0)

lyst loading of 0.05 g and at pH between 6.7 and 7.0. As shown in Fig. 9, the photocatalytic efficiencies have increased with decreases of dye concentrations in the tested solutions for both pure and Zr-doped titania catalysts. When the pure titania was used for the sufficiently low initial CV concentration (the lowest initial concentration was 0.005 mmol/dm^3), the dye was completely degraded after photocatalytic run of 16 h at relatively mild conditions of the UV irradiation (Fig. 9). When the Zr-doped titania was applied, CV dye was degraded during shorter photocatalytic reaction time (inset in Fig. 9.). With the increase of initial CV concentrations, photocatalytic degradation time for both pure and Zr-doped titania decreased (Fig. 9). These observations can be related to the increases in optical densities of the CV dye solutions with the increases of dye concentrations, and subsequent potential restrict of UV irradiation penetrations to the catalysts' surfaces and throughout the test-solutions [36,37].

In all performed photocatalytic runs, the pH of the solutions was between 6.7 and 7.0. Considering that titania is amphoteric and that its zero point charge is at 5.9 [38], the authors predict that the electrostatic attractions between cationic CV dye and negatively charged catalyst surfaces under the applied experimental conditions were driving forces to support the adsorption process of the organic dye and to facilitate further photocatalytic process.

IV. Conclusions

Modified sol-gel method was used as relatively simple procedure for preparing the pure and Zr-doped titania-based nanostructured materials as promising photocatalysts. The photocatalytic efficiencies of both types of catalysts were tested for degradation of the dye CV, under relatively mild operational conditions (low UV irradiation energy, small catalysts dosages and unmodified pH value). The obtained results have indicated that physico-chemical properties of the pure titania were significantly influenced by the doping with zirconium. As a result, doped catalysts have demonstrated significantly higher photocatalytic activity in degradation of CV.

It can be concluded that the achieved bimodal/multimodal distribution of pore sizes as well as higher amount of greater mesopores in size in the case of the Zr-doped titania herein resulted in greater photocatalytic activity. In addition, the presence of mixed crystal phases (anatase, rutile and/or brookite and $ZrTiO_4$) and improved crystalline structure, as well as higher total surface acidity in the case of Zr-doped titania can also be related to more effective photocatalytic activity compared to the pure titania catalyst.

Variations of process parameters showed higher levels of dye degradations with the increases of catalysts dosages and decreases of initial CV concentrations for both catalysts. Longer reaction runs of photocatalytic processes provided higher levels of CV degradations over both catalysts.

The investigated pure titania and particularly titania doped with the optimized content of Zr and calcined at oprimized temperature can be used as promising cost-effective and environmentally friendly catalysts for purification of water(s).

Acknowledgement: The authors wish to thank to the Ministry of Education, Science and Technological Development of the Republic of Serbia (Projects 1612008, 45012, 172061) for financial support.

References

1. H.-J. Fan, C.S. Lu, W.-L.W. Lee, M.-R. Chiou, C.-C. Chen, "Mechanistic pathways differences between P25-TiO_2 and Pt-TiO_2 mediated CV photodegradation", *J. Hazard. Mater.*, **185** (2011) 227–235.
2. C.-C. Chen, W.-C. Chen, M.-R. Chiou, S.-W. Chen, Y. Y. Chen, H.-J. Fan, "Degradation of crystal violet by an FeGAC/H_2O_2 process", *J. Hazard. Mater.*, **196** (2011) 420–425.
3. W.-L. W. Lee, S.-T. Huang, J.-L. Chang, J.-Y. Chen, M.-C. Cheng, C.-C. Chen, "Photodegradation of CV over nanocrystalline bismuth tungstate prepared by hydrothermal synthesis", *J. Mol. Catal. A-Chem.*, **361-362** (2012) 80–90.
4. U. Pagga, K. Taeger, "Development of a method for adsorption of dyestuffs on activated sludge", *Water Res.*, **28** [5] (1994) 1051–1057.
5. C. Hachem, F. Bocquillon, O. Zahraa, M. Bouchy, "Decolourization of textile industry wastewater by the photocatalytic degradation process", *Dyes Pigments*, **49** (2001) 117–125.
6. B. Gao, T.M. Lim, D.P. Subagio, T.-T. Lim, "Zr-doped TiO_2 for enhanced photocatalytic degradation of bisphenol A", *Appl. Catal. A: Gen.*, **375** (2010) 107–115.
7. S.S. Patil, V.M. Shinde, "Biodegradation studies of

aniline and nitrobenzene in aniline plant waste water by gas chromatography", *Environ. Scl. Technol.*, **22** (1988) 1160–1165.
8. A.T. Moore, A. Vira, S. Fogei, "Biodegradation of trans-l,2-dichloroethylene by methane - Utilizing bacteria in an aquifer simulator", *Environ. Sci. Technol.*, **23** [4] (1989) 403–406.
9. R. Jain, M. Shrivastava, "Photocatalytic removal of hazardous dye cyanosine from industrial waste using titanium dioxide", *J. Hazard. Mater.*, **152** (2008) 216–220.
10. L. Andronic, D. Andrasi, A. Enesca, M. Visa, A. Duta, "The influence of titanium dioxide phase composition on dyes photocatalysis", *J. Sol-Gel Sci. Technol.*, **58** [1] (2011) 201–208.
11. G.N. Shao, S.M. Imran, S.J. Jeon, M. Engole, N. Abbas, M.S. Haider, S.J. Kang, H.T. Kim, "Sol-gel synthesis of photoactive zirconia–titania from metal salts and investigation of their photocatalytic properties in the photodegradation of methylene blue", *Powder. Technol.*, **258** (2014) 99–109.
12. D. Kapusuz, J. Park, A. Ozturk, "Sol-gel synthesis and photocatalytic activity of B and Zr co-doped TiO_2", *J. Phys. Chem. Solids*, **74** (2013) 1026–1031.
13. J. Lukáč, M. Klementová, P. Bezdička, S. Bakardjieva, J. Šubrt, L. Szatmáry, Z. Bastl, J. Jirkovský, "Influence of Zr as TiO_2 doping ion on photocatalytic degradation of 4-chlorophenol", *Appl. Catal. B: Environ.*, **74** (2007) 83–91.
14. J. Choina, Ch. Fischer, G.-U. Flechsig, H. Kosslick, V.A. Tuan, N.D. Tuyend, N.A. Tuyen, A. Schulz, "Photocatalytic properties of Zr-doped titania in the degradation of the pharmaceutical ibuprofen", *J. Photoch. Photobio. A*, **274** (2014) 108–116.
15. R.R. Bhosale, S.R. Pujari, G.G. Muley, S.H. Patil, K.R. Patil, M.F. Shaikh, A.B. Gambhire, "Solar photocatalytic degradation of methylene blue using doped TiO_2 nanoparticles", *Sol. Energy*, **103** (2014) 473–479.
16. J. Wang, Y. Lv, L. Zhang, B. Liu, R. Jiang, G. Han, R. Xu, X. Zhang, "Sonocatalytic degradation of organic dyes and comparison of catalytic activities of CeO_2/TiO_2, SnO_2/TiO_2 and ZrO_2/TiO_2 composites under ultrasonic irradiation", *Ultrason. Sonochem.*, **17** (2010) 642–648.
17. M.A. Barakat, G. Hayes, S. Ismat-Shah, "Effect of cobalt doping on the phase transformation of TiO_2 nanoparticles", *J. Nanosci. Nanotechno.*, **5** (2005) 1–7.
18. R. Spurr, H. Myers, "Quantitative analysis of anatase-rutile mixtures with an X-ray diffractometer", *Anal. Chem.*, **29** (1957) 760–761.
19. D. Mardare, A. Manole, A. Yildiz, D. Luca, "Photoinduced wettability of titanium oxide thin films", *Chem. Eng. Comm.*, **198** (2011) 530–540.
20. S. Brunauer, L.S. Deming, W.E. Deming, E. Teller, "On a theory of the Van der Waals adsorption of gases", *J. Am. Chem. Soc.*, **62** (1940) 1723–1732.
21. J.C. Morales-Ortuno, R.A. Ortega-Dominguez, P. Hernandez-Hipolito, X. Bokhimi, T.E. Klimova, "HDS performance of NiMo catalysts supported on nanostructuredmaterials containing titania", *Catal. Today*, **271** (2016) 127–139.
22. S. Bakardjieva, J. Subrt, V. Stengl, M.J. Dianez, M.J. Sayagues, "Photoactivity of anatase–rutile TiO_2 nanocrystalline mixtures obtained by heat treatment of homogeneously precipitated anatase", *Appl. Catal. B: Environ.*, **58** (2005) 193–202.
23. C. Fu, Y. Gong, Y. Wu, J. Liu, Z. Zhang, C. Li, L. Niu, "Photocatalytic enhancement of TiO_2 by B and Zr co-doping and modulation of microstructure", *Appl. Surf. Sci.*, **379** (2016) 83–90.
24. A.L. Castro, M.R. Nunes, A.P. Carvalho, F.M. Costa, M.H. Florencio, "Synthesis of anatase TiO_2 nanoparticles with high temperature stability and photocatalytic activity", *Solid State Sci.*, **10** (2008) 602–606.
25. D.A.H. Hanaor, C.C. Sorrell, "Review of the anatase to rutile phase transformation", *J. Mater. Sci.*, **46** (2011) 855–874.
26. Q. Zhang, L. Gao, J. Guo, "Effects of calcination on the photocatalytic properties of nanosized TiO_2 powders prepared by $TiCl_4$ hydrolysis", *Appl. Catal. B: Environ.*, **26** (2000) 207–215.
27. M.A. Behnajady, H. Eskandarloo, N. Modirshahla, M. Shokri, "Investigation of the effect of sol-gel synthesis variables on structural and photocatalytic properties of TiO_2 nanoparticles", *Desalination*, **278** (2011) 10–17.
28. T. Lopez, R. Gomez, E. Sanchez, F. Tzompantzi, L. Vera, "Photocatalytic activity in the 2,4-dinitroaniline decomposition over TiO_2 sol-gel derived catalysts", *J. Sol-Gel Sci. Technol.*, **22** (2001) 99–107.
29. T. Bezrodna, G. Puchkovska, V. Shimanovska, I. Chashechnikova, T. Khalyavka, J. Baran, "Pyridine-TiO_2 surface interaction as a probe for surface active centers analysis", *Appl. Surf. Sci.*, **214** (2003) 222–231.
30. K.J.A. Raj, B. Viswanathan, "Effect of surface area, pore volume and particle size of P25 titania on the phase transformation of anatase to rutile", *Indian. J. Chem. A*, **48** (2009) 1378–1382.
31. M.D. Hernández-Alonso, I. Tejedor-Tejedor, J. M. Coronado, M. A. Anderson, "Operando FTIR study of the photocatalytic oxidation of methyl cyclohexane and toluene in air over TiO_2–ZrO_2 thin films: Influence of the aromaticity of the target molecule on deactivation", *Appl. Catal. B: Environ.*, **101** (2011) 283–293.
32. F. Fresno, M.D. Hernandez-Alonso, D. Tudela, J.M. Coronado, J. Soria, "Photocatalytic degradation of toluene over doped and coupled $(Ti,M)O_2$ (M = Sn or Zr) nanocrystalline oxides: Influence of the heteroatom distribution on deactivation", *Appl. Catal. B: Environ.*, **84** (2008) 598–606.
33. J.C. Yu, J. Lin, R.W. M. Kwok, "$Ti_{1-x}Zr_xO_2$ solid so-

lutions for the photocatalytic degradation of acetone in air", *J. Phys. Chem. B*, **102** (1998) 5094–5098.
34. X. Fu, L.A. Clark, Q. Yang, M.A. Anderson, "Enhanced photocatalytic performance of titania-based binary metal oxides: TiO_2/SiO_2 and TiO_2/ZrO_2", *Environ. Sci. Technol.*, **30** (1996) 647–653.
35. M.A. Rauf, M.A. Meetani, S. Hisaindee, "An overview on the photocatalytic degradation of azo dyes in the presence of TiO_2 doped with selective transition metals", *Desalination*, **276** (2011) 13–27.
36. Y. Liu, H. Yu, Z. Lv, S. Zhan, J. Yang, X. Peng, Y. Ren, X. Wu, "Simulated-sunlight-activated photocatalysis of methylene blue using cerium-doped SiO_2/TiO_2 nanostructured fibers", *J. Environ. Sci.*, **24** (10) (2012) 1867–1875.
37. R. Kumar, J. Rashid, M.A. Barakat, "Zero valent Ag deposited TiO_2 for the efficient photocatalysis of methylene blue under UV-C light irradiation", *Colloids Interface Sci. Comm.*, **5** (2015) 1–4.
38. M. Kosmulski, "The significance of the difference in the point of zero charge between rutile and anatase", *Adv. Colloids Interface*, **99** (2002) 255–264.